doi:10.1093/jmcb/mjz021
Published online March 29, 2019

Article

A harlequin ichthyosis pig model with a novel *ABCA12* mutation can be rescued by acitretin treatment

Xiao Wang[1,2,8,†], Chunwei Cao[1,8,†], Yongshun Li[1,8], Tang Hai[1,8], Qitao Jia[1,2,8], Ying Zhang[1,2,8], Qiantao Zheng[1,2,8], Jing Yao[1,8], Guosong Qin[1,8], Hongyong Zhang[1,2,8], Ruigao Song[1,2,8], Yanfang Wang[3], Guanghou Shui[4], Sin Man Lam[4], Zhonghua Liu[5,8], Hong Wei[6,8], Anming Meng[7,8], Qi Zhou[1,2,8], and Jianguo Zhao[1,2,8,*]

[1] State Key Laboratory of Stem Cell and Reproductive Biology, Institute of Zoology, Chinese Academy of Sciences, Beijing 100101, China
[2] University of Chinese Academy of Sciences, Beijing 100049, China
[3] State Key Laboratory of Animal Nutrition, Institute of Animal Science, Chinese Academy of Agricultural Sciences, Beijing 100081, China
[4] State Key Laboratory of Molecular Developmental Biology, Institute of Genetics and Developmental Biology, Chinese Academy of Sciences, Beijing 100101, China
[5] College of Life Science, Northeast Agricultural University of China, Harbin 150030, China
[6] Department of Laboratory Animal Science, College of Basic Medical Sciences, Third Military Medical University, Chongqing 400038, China
[7] School of Life Sciences, Tsinghua University, Beijing 100084, China
[8] Chinese Swine Mutagenesis Consortium, Beijing 100101, China
[†] These authors contributed equally to this work.
* Correspondence to: Jianguo Zhao, E-mail: zhaojg@ioz.ac.cn

Edited by Jinsong Li

Harlequin ichthyosis (HI) is a severe genetic skin disorder and caused by mutation in the ATP-binding cassette A12 (*ABCA12*) gene. The retinoid administration has dramatically improved long-term survival of HI, but improvements are still needed. However, the *ABCA12* null mice failed to respond to retinoid treatment, which impedes the development of novel cure strategies for HI. Here we generated an ethylnitrosourea mutagenic HI pig model (named *Z9*), which carries a novel deep intronic mutation IVS49-727 A>G in the *ABCA12* gene, resulting in abnormal mRNA splicing and truncated protein production. *Z9* pigs exhibit significant clinical symptom as human patients with HI. Most importantly, systemic retinoid treatment significantly prolonged the life span of the mutant pigs via improving epidermal maturation, decreasing epidermal apoptosis, and triggering the expression of *ABCA6*. Taken together, this pig model perfectly resembles the clinical symptom and molecular pathology of patients with HI and will be useful for understanding mechanistic insight and developing therapeutic strategies.

Keywords: harlequin ichthyosis, *ABCA12*, pig model, acitretin, ENU mutagenesis, deep intronic mutation

Introduction

Harlequin ichthyosis (HI) is an inherited disease, which mainly affects the skin. HI is the most severe form of autosomal recessive congenital ichthyosis (ARCI), which includes HI, congenital ichthyosiform erythroderma, and lamellar ichthyosis (Akiyama and Shimizu, 2008). Patients with HI are born with a thick covering of armor-like scales over the entire body. Affected infants also have abnormal facial features, including ectropion, eclabium, and flattening of the ears and nose (Farhadi and Kazemi, 2013; Parikh et al., 2016). According to clinical data of 45 patients with HI, the ages of the survivors ranged from 10 months to 25 years, with an overall survival rate of 56% (Rajpopat et al., 2011). Most infants died from microbial infections, feeding problems or respiratory distress. The survival rate of patients with HI increased to ~80% after being treated with systemic retinoids, which is an anchor therapy in disorders of keratinization (Rajpopat et al., 2011). Therefore, a more comprehensive therapeutic protocol for this disease is still under development, which certainly relies on

Received January 8, 2019. Revised February 20, 2019. Accepted March 8, 2019.

obtaining more clear understanding of pathological mechanism with the aid of optimal animal models.

Two independent research groups have reported that the *ABCA12* gene is the causative gene of HI (Akiyama et al., 2005; Kelsell et al., 2005). The *ABCA12* gene belongs to ATP-binding cassette (ABC) transporter superfamily (Annilo et al., 2002; Lefvre et al., 2003); the *ABC* genes encode a large number of membrane proteins involved in energy-dependent transport of various substrates across cell membranes, and mutations in these genes cause several human genetic disorders (Allikmets et al., 1996; Dean and Allikmets, 2001). The ABCA12 protein is located within the lamellar granules (LGs) in the epidermal keratinocytes and is supposed to be involved in lipid transport into the extracellular space. LGs, also called lamellar bodies, are specialized vesicular structures in the cytoplasm, which function to transport lipids to extracellular space (Sakai et al., 2007). ABCA12 thus plays a critical role in transporting lipids within the epidermal cells and formation of the intercellular lipid layer, ultimately influencing the epidermal barrier function.

Three independent research groups have generated *ABCA12* null mice by either ethylnitrosourea (ENU) mutagenesis or homologous recombination (Smyth et al., 2008; Yanagi et al., 2008; Zuo et al., 2008). These models partially reproduce the human HI skin phenotype and aid the investigation of pathological mechanisms of HI due to *ABCA12* deficiency. However, even treated with fetal retinoid, all *ABCA12* null mice die within a few hours of birth, showing neither improved skin phenotype nor extended survival period (Yanagi et al., 2008). This situation severely limits the use of mouse model for guiding the development of innovative treatments, including new drugs and nursing methods, for ichthyosis with *ABCA12* deficiency.

Pigs and humans share numerous similarities in genetics, anatomy, physiology, pathology, and immunology (Swindle et al., 2012; Lin et al., 2017), which make pigs very suitable for modeling many human diseases. The structure and physiology of porcine and human skin are very similar, which make pigs a useful model to study human skin related diseases (Debeer et al., 2013; Summerfield et al., 2015). Till now, many pig models have been developed and used in human skin-related studies, including wound repair (Ansell et al., 2012), burn research (Abdullahi et al., 2014), infectious diseases (Meurens et al., 2012), as well as chemical penetration studies (Barbero and Frasch, 2009).

In the current study, we created a novel ENU-induced deep intronic mutation IVS49-727 A>G in the *ABCA12* gene that results in abnormal mRNA splicing and truncated protein production, causing hyperkeratotic skin in Bama miniature pigs. The affected (named *Z9* later) pigs show pathological features as human patients with HI. Most importantly, therapeutic effects were observed in pigs treated with systemic retinoids therapy. These pigs provide a remarkable model of human HI to better understand the pathological mechanisms of this disease and develop novel prevention and treatment strategies.

Results

Pig mutants presented with sclerotic, dry, and chapped skin, which mimic symptoms of human HI

The *Z9* mutants were identified in a three-generation breeding scheme based on a large-scale screen of ENU-mutagenized porcine populations (Hai et al., 2017a). Affected G3 offspring were generated by backcrossing G2 sows with a G1 founder, and *Z9* pigs were identified with sclerotic, dry, and chapped skin (Figure 1A). Ectropion, eclabium, flattening ears, decreased activities, and neonatal death were also observed in *Z9* pigs. Furthermore, the birth weight of *Z9* pigs was significantly lower than that of wild type (WT) littermates (WT, 0.51 ± 0.13 kg, $n = 51$; *Z9*, 0.39 ± 0.10 kg, $n = 18$; $P < 0.001$; Supplementary Figure S1).

To investigate the pathological changes of *Z9* skin, skin samples were collected for histological analysis. Histological sections from the skin of neonatal *Z9* pigs revealed markedly hyperkeratotic stratum corneum (SC), as well as a lack of normal skin folds (Figure 1B). The spinous cells and basale cells of the skin from *Z9* pigs also exhibited abnormal arrangement. These characteristics of skin from *Z9* pigs are consistent with those from patients with HI.

Transmission electron microscopy (TEM) was performed to investigate the ultrastructure defects in the skin tissue of neonatal *Z9* pigs. Clear lipid lamellar structures in the SC of WT skin were observed. In contrast, *Z9* pigs were observed to have massive hyperkeratotic SC, losing normal lamellar structures in the interstitial spaces (Figure 1C). The WT stratum granulosum (SG) showed numerous LGs with typical structure and some LGs are close to interstitial lamellar structures, while the *Z9* cytoplasm of the SG showed plenty of multivesicular bodies instead of normal LGs.

To examine the SC, cornified envelopes were isolated from epidermis of WT and newborn *Z9* pigs and then photographed under a light microscope. Cornified envelopes were prepared as previously described (Koch et al., 2000). *Z9*-cornified envelopes exhibit several defects in comparison with those of WT pigs (Figure 1D). In detail, cornified envelopes from *Z9* pigs showed more irregular and fragile appearance, while those from WT pigs showed mature and rigid appearance. In addition, *Z9*-cornified envelopes tended to stack up, while cornified envelopes from WT pigs had smooth surface and were neatly arranged in liquid.

Since severe dehydration was observed in *Z9* carcasses, the barrier function of the epidermis was investigated, and skin permeability assay was carried out. Euthanized neonatal pigs were stained with toluidine blue and washed with phosphate buffered saline (PBS). Results showed that the skin of neonatal *Z9* pigs had increased inward permeability to toluidine blue (Figure 1E). A gravimetric transepidermal water loss (TEWL) assay, which is able to measure water evaporation from the skin surface, was performed on samples harvested from neonatal pig dorsal skin and abdominal skin. Water loss of the *Z9* skin was significantly higher than that of WT skin at any time point (Figure 1F). These results indicate that the epidermal permeability barrier was disrupted in *Z9* pigs.

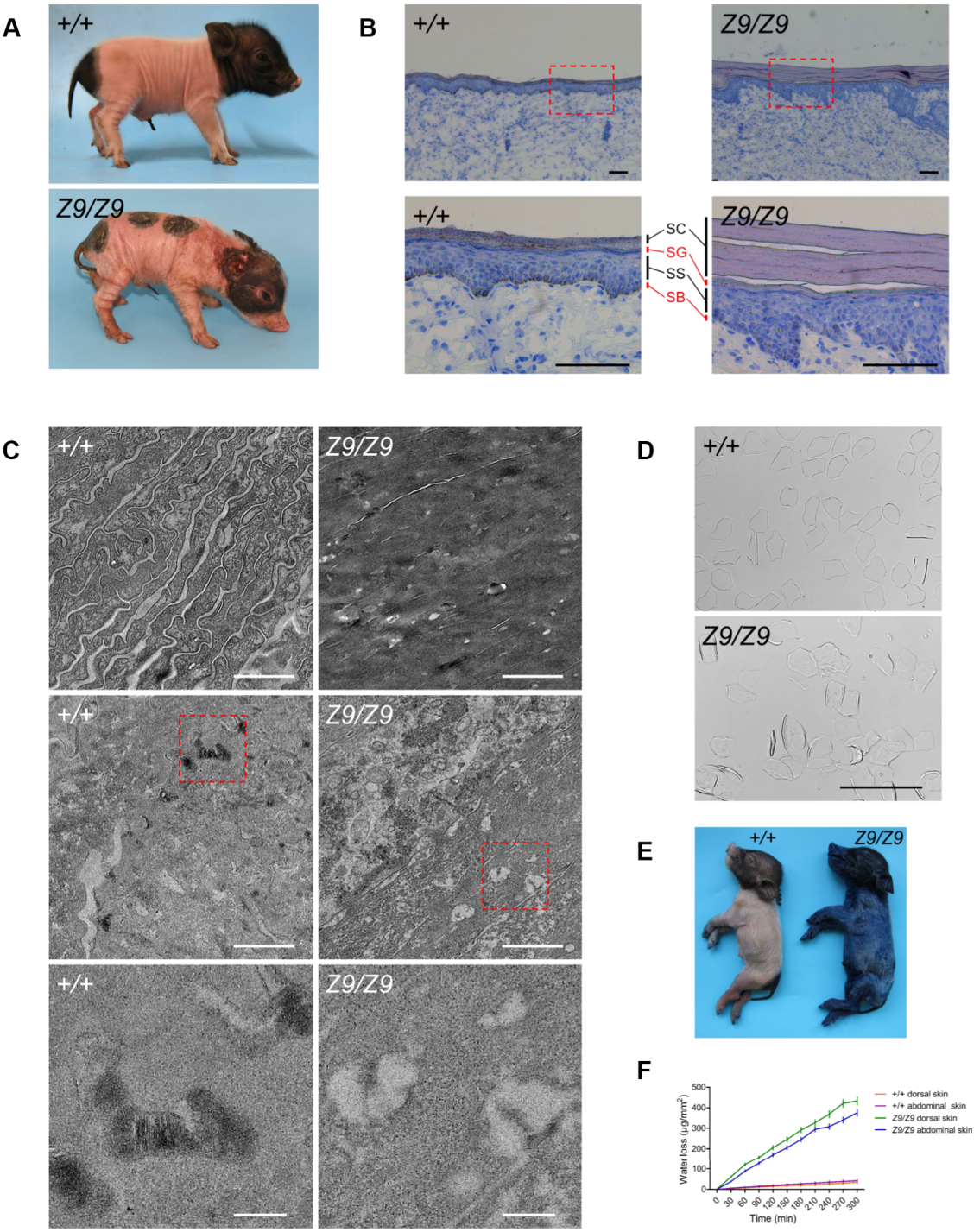

Figure 1 Skin phenotype of an ENU-induced pig disease model. (**A**) Newborn *Z9* pigs displayed a phenotype of sclerosis, dry and chapped skin, and neonatal death. (**B**) Histological sections of epidermis of neonatal *Z9* pigs exhibited hyperkeratotic SC, lack of normal skin folds, and disordered SS. The lower panels show the magnified images of the selected region (red frames) of upper panels. Scale bar, 100 μm. (**C**) Ultrastructural defects in the epidermis of *Z9* pigs were observed by TEM, including massive hyperkeratotic structure in the SC (top) and numerous multivesicular bodies in the SG (middle and bottom). Scale bar, 1 μm (top and middle) and 200 nm (bottom). The bottom panels show the magnified images of the selected region (red frames) of middle panels. (**D**) Cornified envelopes isolated from newborn *Z9* pigs were irregular and fragile compared with WT controls. Scale bar, 100 μm. (**E**) Toluidine blue staining of euthanized neonatal *Z9* pigs shows defects in epidermal barrier function. (**F**) The TEWL assay shows a defect in barrier formation of the dorsal and abdominal skin from *Z9* pigs ($n = 4$; $P < 0.05$ between WT and *Z9* pigs).

Mapping and identification of the causative mutation in ABCA12 gene

The mutant phenotype was not observed in G1 and G2 pigs but was discovered in both male and female G3 pigs (Figure 2A). Among 50 offspring from 7 litters, 37 WT pigs and 13 mutant pigs were identified, with a ratio of ~3:1 (Figure 2B). These data implied that the mutation in the *Z9* mutant pedigree is inherited in an autosomal recessive manner.

To identify the causative mutation in the *Z9* mutant pedigree, a family-based genome-wide association study (GWAS) and candidate gene sequencing were performed. GWAS results showed a strong signal at 119 Mb to 133 Mb on chromosome 15 (Supplementary Figure S2). Similarly, the linkage analysis also identified the significant linkage signal of a 19 Mb region on chromosome 15 between 120 Mb and 139 Mb (Figure 2C). There are 38 annotated genes (Supplementary Table S1) in the overlapped genomic interval (120 Mb–133 Mb). Among these genes, *ABCA12*, whose mutations are known to result in ARCI, was selected for mutation screening.

Sanger sequencing of all 53 exons of *ABCA12* revealed that no mutation co-segregated with *Z9* phenotype in this pedigree. In order to determine if there was abnormal splicing of the *ABCA12* gene in *Z9* pigs, the mRNA was amplified and sequenced using a series of primer sets (Supplementary Table S2) that allows complete analysis of 7788 bp coding sequences (CDSs) of *ABCA12* gene in overlapping fragments. An unexpected length of polymerase chain reaction (PCR) products amplified by CDS-11 primers was observed in *Z9* pigs (Figure 2D), and sequencing results showed a splicing alteration of mRNA with a 132-nt insertion between exon 49 and exon 50 in *Z9* pigs (Figure 2E). The 132-nt insertion in *ABCA12* mRNA of *Z9* pigs was mapped to intron 49 of the *ABCA12* gene by basic local alignment search

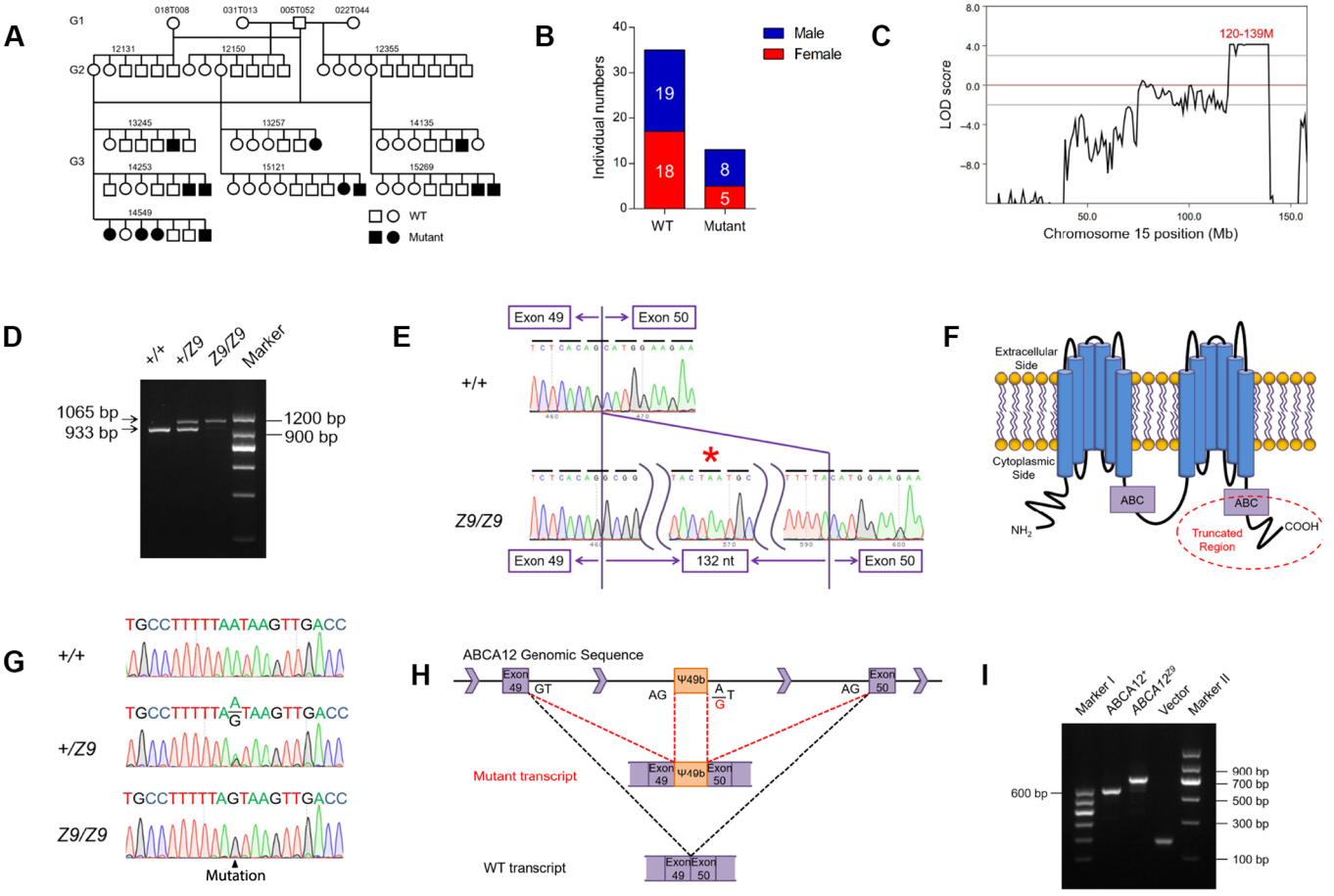

Figure 2 and identification of the novel *ABCA12* mutation. (**A**) Pedigree map shows the autosomal recessive inheritance of the *Z9* mutation. (**B**) Distribution of the number of WT and mutant pigs in the G3 offsprings. (**C**) Through genetic linkage analysis, only one linkage signal (LOD, 4.13) among the whole genome was identified in a 19 Mb region on chromosome 15. (**D**) Reverse-transcription PCR indicated abnormal pre-mRNA splicing. (**E**) Sequencing of *ABCA12* mRNA revealed a 132-nt insertion in *Z9* pigs, which introduced a premature stop codon. The red asterisk indicates stop codon (UAA). (**F**) *ABCA12* with the *Z9* mutation expresses a truncated protein, which lacked part of its ABC domain. (**G**) A deep intronic mutation of IVS49-727 A>G in *ABCA12* results in splicing alteration. (**H**) Brief summary of gene mapping: a deep intronic mutation in *ABCA12* was located. (**I**) Minigene experiment was carried out to verify the effect of the *ABCA12* IVS49-727 A>G mutation on pre-mRNA splicing *in vitro*.

tool (BLAST). The insertion introduced a premature stop codon, resulting in the expression of a truncated ABCA12 protein that lacked the second ABC domain (Akiyama, 2010; Figure 2F). In order to identify the causative mutation that results in the splicing alteration, the whole intron 49 was sequenced in *Z9* pigs. As expected, a deep intronic mutation of A to G (IVS49-727 A>G) was identified next to the 3′ end of the insertion sequence in *Z9* pigs (Figure 2G). According to the GT–AG rule, this mutation leads to a new splicing site and produces a 132-nt pseudoexon (named Ψ49b) (Figure 2H). The IVS49-727 A>G mutation in *ABCA12* was only found in *Z9* pedigree rather than in the SNP database or commercial pig breeds (Supplementary Table S3), indicating that this mutation might be the causative mutation and induced by ENU mutagenesis.

To assess if the IVS49-727 A>G mutation affects *ABCA12* pre-mRNA splicing directly, we constructed WT and *Z9* minigenes containing the genomic sequence from exon 49 to exon 50 of *ABCA12* and transfected minigenes into 293T cells. The results showed that the IVS49-727 A>G mutation from *Z9* pigs caused alterations in pre-mRNA splicing, similar to that seen *in vivo* (Figure 2I). Taken together, these data indicate that the IVS49-727 A>G mutation in *ABCA12*, which resulted in a 132-nt insertion in mature mRNA, was the causative mutation of *Z9* pigs.

Interestingly, we have observed that the PCR product of *Z9* mRNA contained minor bands that are shorter than the main band, which indicates that more splicing isoforms were produced by the mutation (Figure 2D). Sequencing results of the minor bands showed that *ABCA12* gene with IVS49-727 A>G mutation also contains WT transcript and two other abnormally spliced transcripts (mutant transcripts 2 and 3) containing different exon skipping (Supplementary Figure S3A). Real-time quantitative PCR (RT-qPCR) results showed that the WT transcript expression level in *Z9* skin is only 1/36 of that in WT skin and most of the *ABCA12* expressions are alternative splicing isoforms (Supplementary Figure S3B).

IVS49-727 A>G mutation in ABCA12 causes abnormal skin lipid composition and increased lipid accumulation

As ABCA12 is a lipid transporter involved in lipid transport from cytoplasm to the extracellular space, lipidomics analysis was performed to investigate the effects of the *ABCA12* IVS49-727 A>G mutation on lipid composition in porcine skin (Supplementary Table S4). Significantly different lipidomic profile of WT and *Z9* skins was observed, suggesting that *ABCA12* IVS49-727 A>G mutation should disrupt lipid transport process in $ABCA12^{Z9/Z9}$ skins (Figure 3A). Heatmap revealed that the mass levels of lipid species were significantly different between WT and *Z9* skin ($P < 0.05$; Figure 3B). The significantly altered lipid subclasses account for 49.9% (190/381) of total subclasses. Besides the significantly decreased diacylglycerides, triacylglycerides, significantly increased levels of ceramide (Cer) were detected in skin tissues of *Z9* pigs, which were consistent with reports in mice (Smyth et al., 2008). Glucosylceramides (GluCer) rather than galactosylceramides were markedly increased. Sphingosines (Sph), a breakdown product of Cer, and free cholesterols were also significantly increased (Figure 3C). To confirm the impaired lipid transport of *Z9* pigs *in vitro*, $ABCA12^{+/+}$, $ABCA12^{+/Z9}$, and $ABCA12^{Z9/Z9}$ fibroblasts were cultured in the presence of acetylated low-density lipoprotein (AcLDL) as the donor of lipid and the liver X receptor (LXR) agonist TO-901317 as the activator of the *ABCA12* gene. The oil red O staining revealed that the lipid accumulation in $ABCA12^{Z9/Z9}$ fibroblasts was notably higher than that observed in $ABCA12^{+/+}$ and $ABCA12^{+/Z9}$ fibroblasts (Figure 3D and E). Taken together, these data indicated that the lipid homeostasis is disrupted in the skin of *Z9* pigs, suggesting that *ABCA12* is not only involved in the transport of lipids in skin but also plays a wider role in lipid metabolism.

Oral administration of acitretin improves the skin condition and survival rate of Z9 pigs

Acitretin, a synthetic retinoid, has been reported to be effective for the survival of patients with HI (Singh et al., 2001); however, the therapy neither improved skin manifestations nor extended the survival of mice used as an HI disease model (Farhadi and Kazemi, 2013). In order to investigate whether the porcine HI model responds to acitretin treatment, oral administration of acitretin to the pregnant sow (10 mg/kg daily; 30 consecutive days) and neonatal *Z9* pigs (1 mg/kg daily; from the first day of birth) were carried out. As a result of acitretin treatment to the sow, neonatal *Z9* pigs achieved significant improvement in the skin phenotype at birth (Figure 4A), and no fissures were observed over the whole body. Most importantly, acitretin treatment to the *Z9* pigs resulted in extension of the survival period from 2 days to at most 23 days (mean ± SD: survival time, 7 ± 9 days, $n = 5$). In contrast, *Z9* pigs without treatment survived no more than 48 h even with intensive care (Figure 4B). Histology results also showed improvement of skin condition in *Z9* pigs with acitretin treatment (Figure 4C). The SC of *Z9* pigs with treatment was slightly thinner than that without treatment, while the stratum basale (SB) of *Z9* pigs with treatment was more like that of normal epidermis.

Acitretin treatment improves the terminal differentiation of epidermis in Z9 pigs

To investigate the lipid barrier function of the epidermis, double immunofluorescent labeling of GluCer and Cer was performed on the skin from $ABCA12^{+/+}$ pigs, $ABCA12^{Z9/Z9}$ pigs, and treated $ABCA12^{Z9/Z9}$ pigs. Cer was evenly distributed in the entire epidermis of $ABCA12^{+/+}$ pigs, including the SC, but hardly distributed in the SC of $ABCA12^{Z9/Z9}$ pigs. GluCer showed intensive distribution in the SC of $ABCA12^{+/+}$ pigs but showed slight staining in that of $ABCA12^{Z9/Z9}$ pigs. It suggests that lipid barrier was disrupted in the *Z9* epidermis. The $ABCA12^{Z9/Z9}$ pigs achieved partial improvement of GluCer distribution after treatment, which was more like the staining pattern of $ABCA12^{+/+}$ pigs. It suggests that the lipid barrier function in the epidermis of $ABCA12^{Z9/Z9}$ pigs was partially restored after acitretin treatment (Figure 5A).

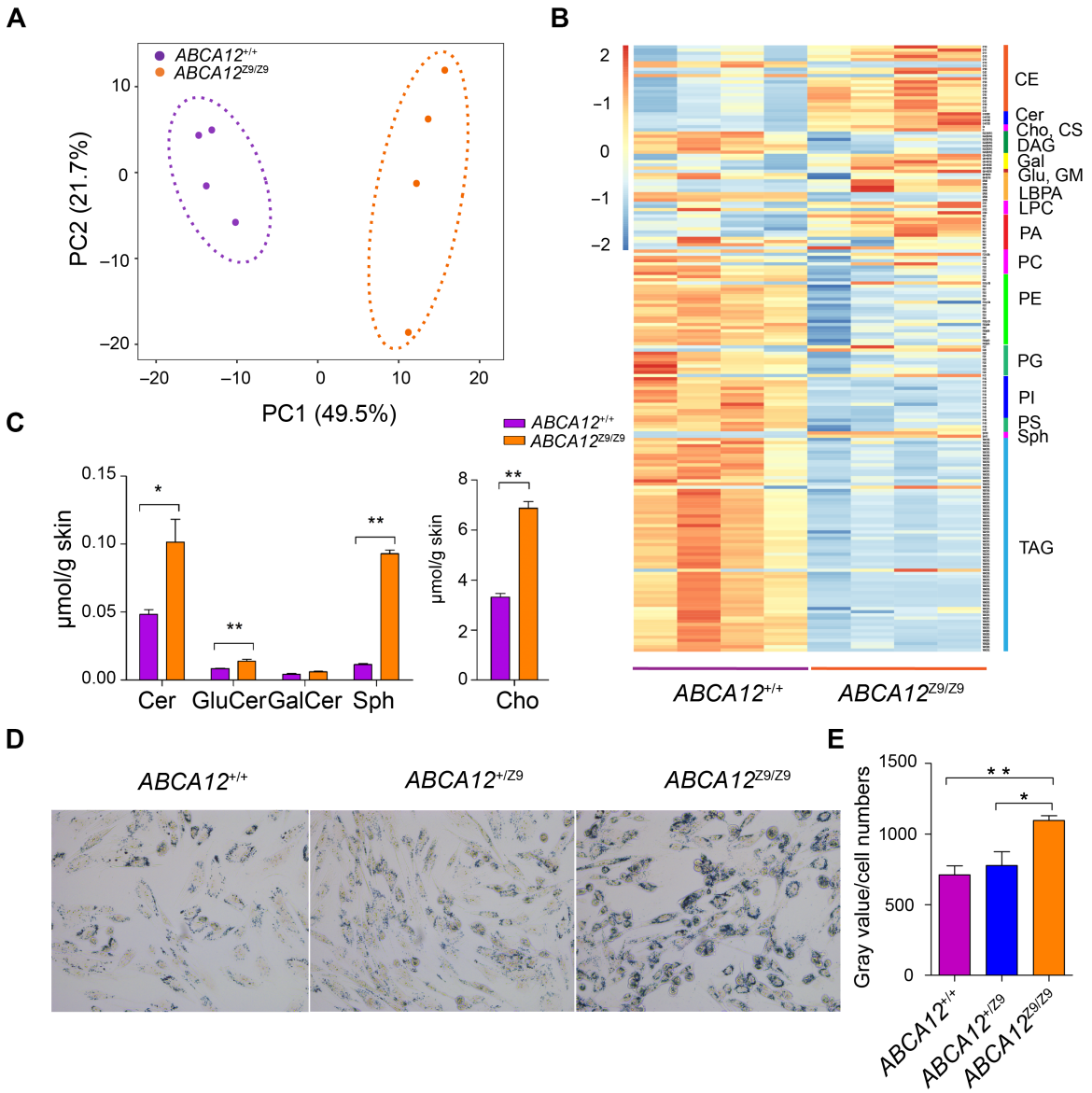

Figure 3 *ABCA12* mutation impacts lipid homeostasis. (**A**) Principal component analysis score plot of lipidomic profile of four paired WT and *Z9* skin. (**B**) Heatmap revealed the mass level of lipid species, which showed significantly different between WT and *Z9* skin ($P < 0.05$). CE, cholesteryl esters; Cer, ceramide; Cho, free cholesterol; CS, cholesteryl sulfate; DAG, diacylglycerides; GalCer, galactosylceramides; GluCer, glucosylceramides; GM, monosialo-dihexosyl gangliosides; LBPA, lyso-bisphosphatidic acids; LPC, lyso-PG; PA, phosphatidic acids; PC, phosphatidylcholines; PE, phosphatidylethanolamines; PG, phosphatidylglyerols; PI, phosphatidylinositols; PS, phosphatidylserines; Sph, sphingosines; TAG, triacylglycerides. (**C**) In the skin of *Z9* pigs, the levels of ceramide, GluCer, Sph, and Cho were significantly increased compared with WT controls (*$P < 0.05$, **$P < 0.01$). (**D**) The lipid accumulation in *ABCA12*$^{Z9/Z9}$ fibroblasts was greater than that in *ABCA12*$^{+/+}$ and *ABCA12*$^{+/Z9}$ fibroblasts. Scale bar, 100 µm. (**E**) Quantitative analysis for **D** indicated that gray values per cell in *ABCA12*$^{Z9/Z9}$ fibroblasts were higher than those in *ABCA12*$^{+/+}$ and *ABCA12*$^{+/Z9}$ fibroblasts ($n = 3$; *$P < 0.05$, **$P < 0.01$).

The lipid barrier function of epidermis relies on ABCA12 protein. In WT pigs, the ABCA12 protein was primarily detected in the stratum spinosum (SS) of the epidermis, while the protein was concentrated in the upper SS in the *ABCA12*$^{Z9/Z9}$ epidermis, suggesting perturbed location of the ABCA12 protein. After treatment with acitretin, the distribution of ABCA12 protein in *ABCA12*$^{Z9/Z9}$ pigs shows a pattern similar to that in WT pigs (Figure 5B).

The epidermis of *ABCA12*$^{+/+}$ and *ABCA12*$^{Z9/Z9}$ pigs show different differentiation features. Keratin 14 (K14), a marker of SB cells, was detected in the lowest cellular layer of the epidermis with a regular outline of the SB in *ABCA12*$^{+/+}$ pigs. In the *ABCA12*$^{Z9/Z9}$ epidermis, K14 expression was also in the lowest cellular layer but show a disordered outline of the SB. The disordered outline of the SB was greatly improved in the epidermis of *ABCA12*$^{Z9/Z9}$ pigs after treatment, and the K14 expression was

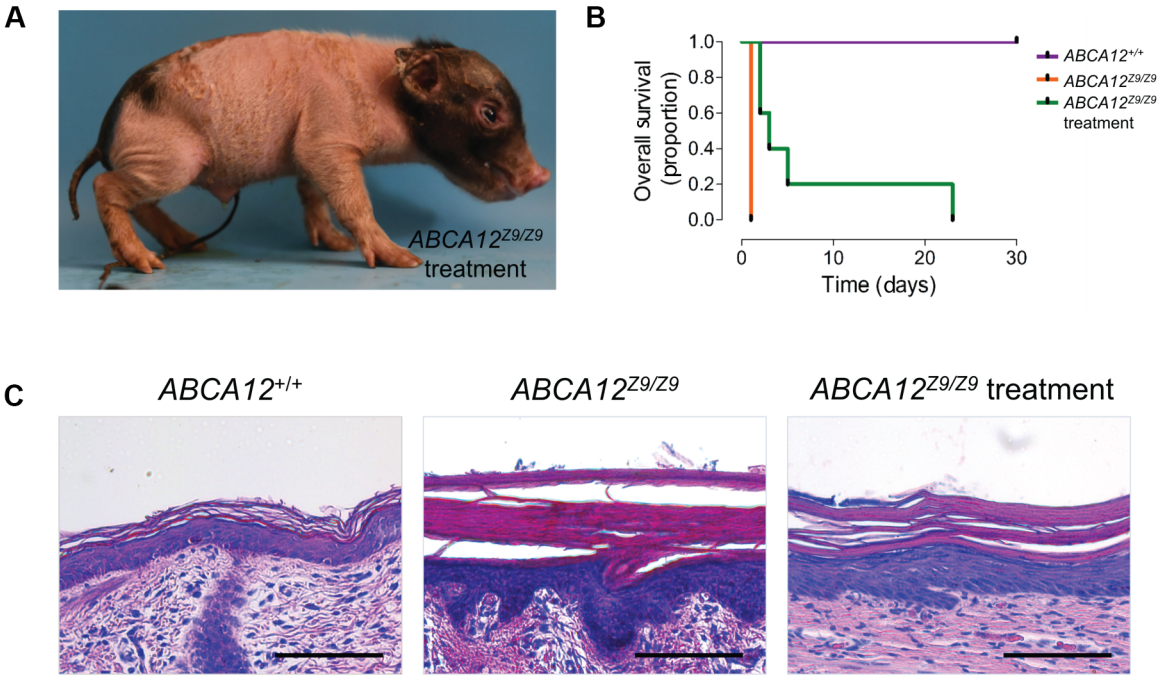

Figure 4 Oral administration of acitretin improves the survival rate of *Z9* pigs. (**A**) *Z9* pigs achieved significant improvement in the skin phenotype at birth with oral administration of acitretin to the pregnant sow (10 mg/kg daily; 30 consecutive days) and neonatal *Z9* pigs (1 mg/kg daily; from the first day of birth). (**B**) Acitretin treatment to the *Z9* pigs extended the survival period from 3 days to 23 days (*ABCA12*$^{+/+}$: $n = 20$; *ABCA12*$^{Z9/Z9}$: $n = 6$; *ABCA12*$^{Z9/Z9}$ with treatment: $n = 5$). (**C**) The histologic sections showed an improvement of skin SC and SB. The SB of *Z9* pigs with treatment was more like that of normal epidermis. Scale bar, 100 μm.

more expansive (Figure 5C). Keratin 10, a marker of epidermal differentiation, was expressed sparsely in the SS and intensely in the SC. However, a defect of epidermal differentiation with hyperkeratinization was observed in *ABCA12*$^{Z9/Z9}$ pigs and this condition was improved by acitretin treatment (Figure 5D). Loricrin, a terminal differentiation marker and a major protein component of the cornified cell envelope (Yoneda and Steinert, 1993), was intensely expressed in the SG of the epidermis from *ABCA12*$^{+/+}$ pigs, while loricrin was diffusely expressed in the whole SC and SG of the epidermis from *ABCA12*$^{Z9/Z9}$ pigs. However, in *ABCA12*$^{Z9/Z9}$ pigs treated with acitretin, loricrin showed a similar expression pattern as WT pigs (Figure 5E). Filaggrin, which is cross-linked to the cornified envelope, participates in coordinating the structure of the cornified cells (Steinert and Marekov, 1995). We also characterized filaggrin to further evaluate the cornified cell envelope. In the epidermis, filaggrin was expressed diffusely in the SS of *ABCA12*$^{Z9/Z9}$ pigs, whereas treatment with acitretin led to the intense expression of filaggrin in the SC and SG, resembling expression levels seen in *ABCA12*$^{+/+}$ pigs (Figure 5F). We assessed cellular proliferation by staining the proliferation marker Ki67 (Supplementary Figure S4). Ki67 was observed in the basal layers of the porcine epidermis. The ki67 positive cells of *ABCA12*$^{+/+}$, *ABCA12*$^{Z9/Z9}$, and treated *ABCA12*$^{Z9/Z9}$ epidermis were about an equal number.

Terminal deoxynucleotidyl transferase-mediated dUTP nick-end labeling (TUNEL) assays were performed to investigate cell apoptosis in the skin (Figure 5G). It is detected that *ABCA12*$^{Z9/Z9}$ epidermis exhibited premature apoptosis in the spinosum and granular layers compared with that of *ABCA12*$^{+/+}$, while *ABCA12*$^{Z9/Z9}$ with treatment epidermis exhibited less expansive TUNEL staining than that of *ABCA12*$^{Z9/Z9}$. It was reported that the activation of the AKT signal pathway have an antiapoptotic function, and the level of Ser-473 phosphorylated AKT in the Abca12$^{-/-}$ mouse was higher than those of control mice (Yanagi et al., 2011). In the current study, we assessed the degree of AKT activation in *Z9* skin before and after acitretin treatment by immunoblot analysis. Oppositely, the skin of *Z9* pigs showed lower expression levels of phosphorylated AKT than those of the WT pigs (Supplementary Figure S5A and B).

ABCA6 expression is upregulated in acitretin-treated Z9 pigs

To better understand the pathogenesis underlying HI caused by *ABCA12* mutations and the therapeutic mechanism of acitretin on HI, RNA sequencing (RNA-seq) analysis was performed to identify the transcriptional profiles in the skin from three groups of pigs. The differentially expressed genes (DEGs) were screened based on the criteria of false discovery rate (FDR)-value <0.05 and absolute fold change ≥ 2. The volcano plots showed a broad overview of the DEGs in the skin of WT vs. *Z9* pigs (Figure 6A) as well as *Z9* pigs vs. treated *Z9* pigs (Figure 6B). Our results indicated that 1272 upregulated genes and 1887 downregulated genes were found in *Z9* pigs, and 639 upregulated genes and 402 downregulated genes were found in *Z9* pigs

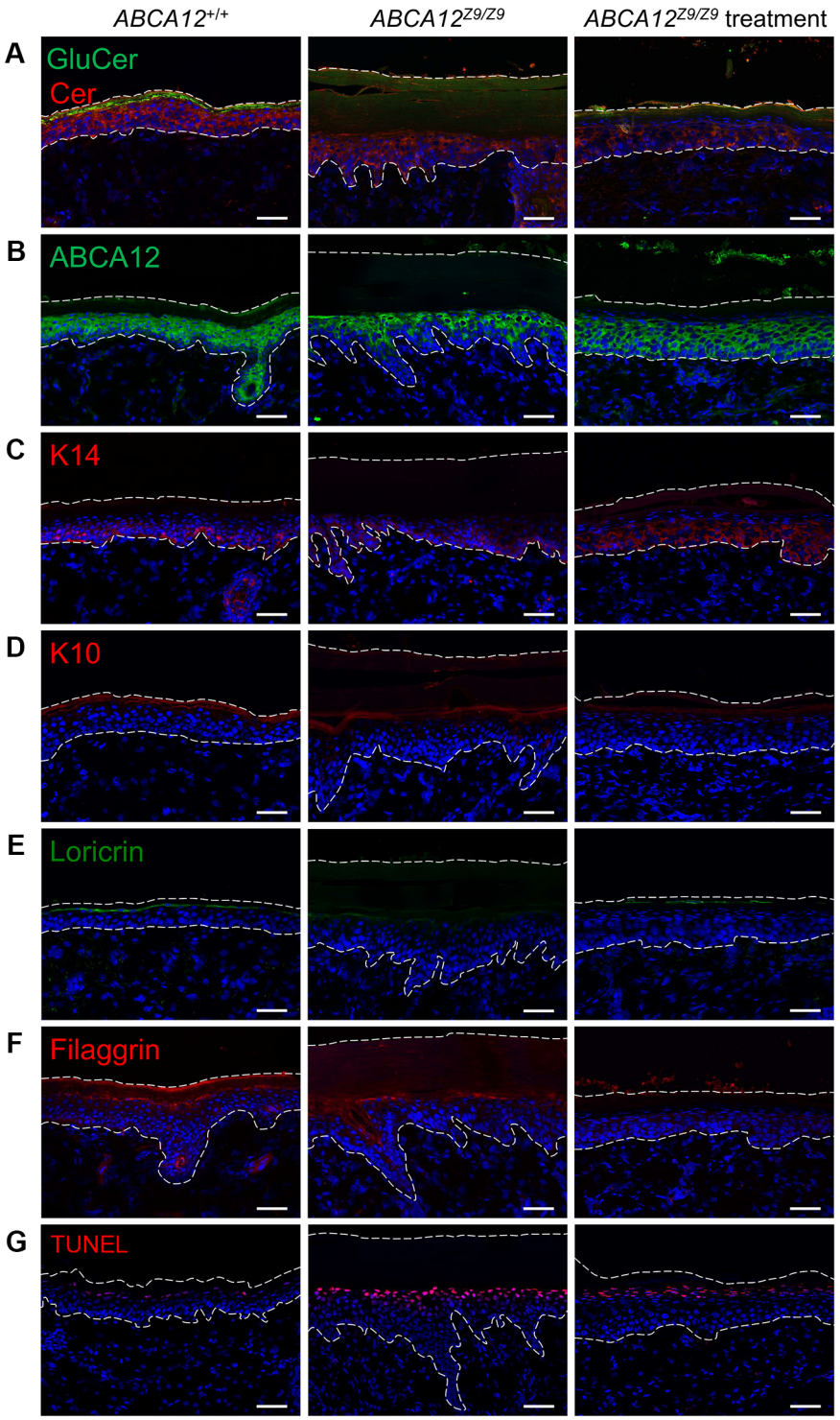

Figure 5 Acitretin treatment improved the terminal differentiation of *Z9* skin. (**A**) Immunofluorescence staining demonstrated the deficiency of both Cer and GluCer in the SC of *ABCA12*$^{Z9/Z9}$ pigs. (**B**) The ABCA12 protein was primarily detected in the SS of WT pigs but was concentrated in the upper SS in the *ABCA12*$^{Z9/Z9}$ epidermis. After acitretin treatment, ABCA12 protein in *ABCA12*$^{Z9/Z9}$ pigs was distributed in a pattern similar to that in WT pigs. (**C**) The disordered outline of K14 in the SB was greatly improved in the epidermis of *ABCA12*$^{Z9/Z9}$ pigs after treatment. (**D–F**) Staining for K10 as well as the cornified envelope marker loricrin and filaggrin showed diffuse expression in the SC *ABCA12*$^{Z9/Z9}$ pigs, revealing abnormal differentiation of keratinocytes. (**G**) *ABCA12*$^{Z9/Z9}$ epidermis exhibited premature apoptosis in the spinosum and granular layers. The cell nuclei were counterstained with Hoechst 33342 (blue). Scale bar, 50 μm.

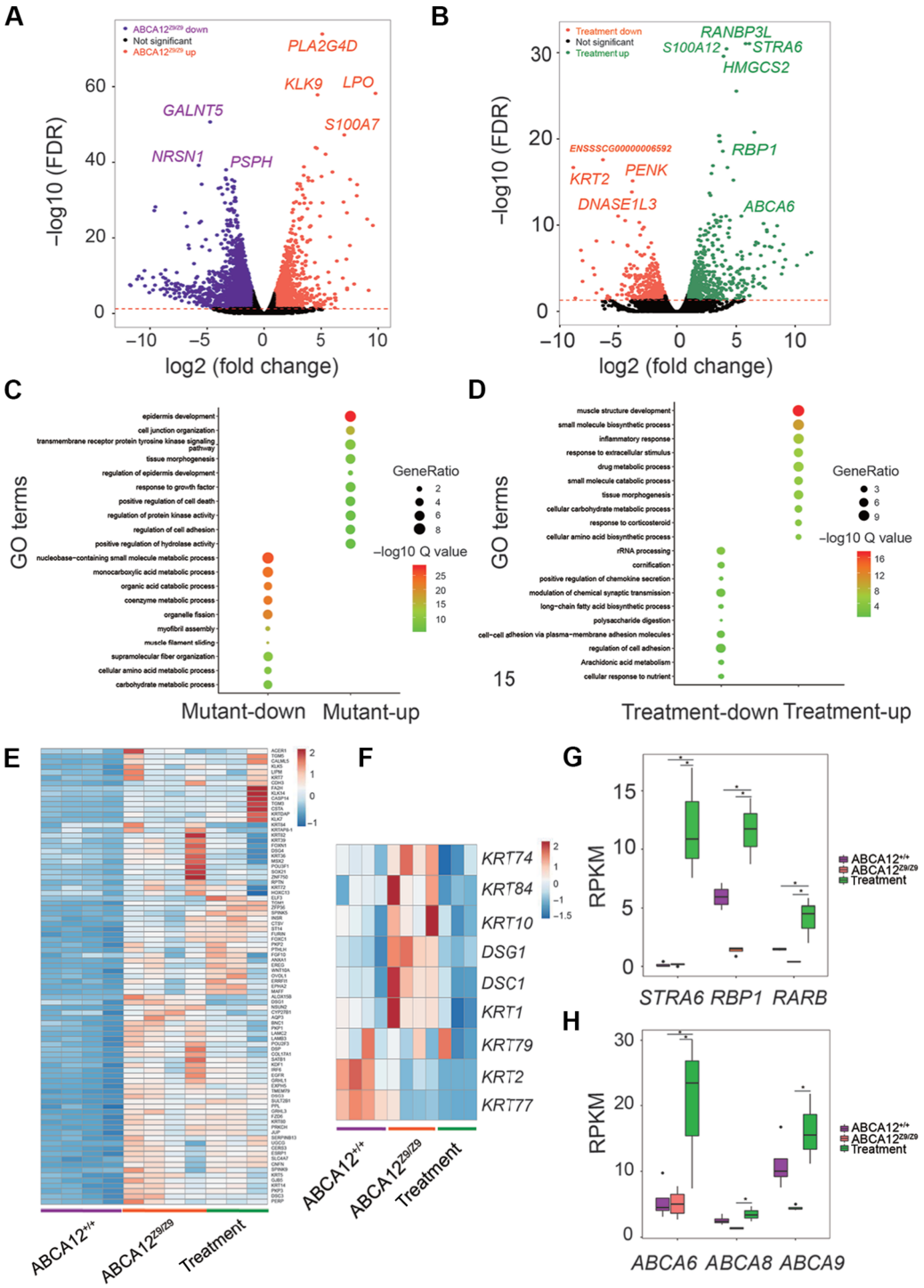

Figure 6 Transcriptome analysis of the skin tissue of WT, *Z9*, and treated *Z9* pigs. (**A**) The volcano plot revealed a broad overview of the difference in gene expression between WT and *Z9* pigs. (**B**) The volcano plot revealed a broad overview of the difference in gene expression between *Z9* pigs and *Z9* pigs treated with acitretin. (**C**) Functional enrichment analysis of upregulated and downregulated DEGs in *Z9* pigs compared with WT pigs identified the significantly overrepresented GO terms (corrected $P < 0.05$). (**D**) Functional enrichment analysis of upregulated and downregulated DEGs in acitretin-treated *Z9* pigs compared with *Z9* pigs identified significantly enriched GO terms (corrected $P < 0.05$). (**E**) Heatmap showed the upregulated expression of genes in GO term of epidermis development (GO:0008544) in *Z9* pigs. (**F**) Heatmap showing the downregulated expression of genes in GO term of cornification (GO:0070268) after acitretin treatment of *Z9* pigs. (**G**) mRNA abundance determined by RNA-seq showed that *STRA6*, *RBP1*, and *RARB* expressions were notably increased (FPKM) after acitretin treatment ($n = 3$; $P < 0.05$). (**H**) mRNA abundance determined by RNA-seq showed that *ABCA6*, *ABCA8*, and *ABCA9* expression levels were notably increased after acitretin treatment ($n = 3$; $P < 0.05$).

with acitretin treatment. Moreover, 15 top DEGs were selected and verified by RT-qPCR (Supplementary Figure S6A and B).

The functional enrichment analysis identified the upregulated epidermis development (GO:0008544) as the most significantly enriched gene ontology (GO) term, indicating epidermis development of *Z9* pigs were disrupted (Figure 6C and E). Interestingly, we also found that genes in GO term of cornification (GO:0070268) were significantly downregulated after acitretin treatment of *Z9* pigs, suggesting that acitretin treatment partially restore the epidermis development in *Z9* pigs (Figure 6D and F).

Among these top DEGs, three genes related to retinol metabolism were identified, including *STRA6* (FDR, 9.04×10^{-32}; $\log_2$ fold change, 6.1), which encodes a membrane protein involved in the metabolism of retinol; *RBP1* (FDR, 1.06×10^{-13}; $\log_2$ fold change, 2.97), which encodes the carrier protein involved in the transport of retinol; and *RARB* (FDR, 3.23×10^{-8}; $\log_2$ fold change = 2.75), which is a nuclear transcriptional regulators in cytoplasm (Figure 6G). This result implied that the oral administration of acitretin induced the response of retinol metabolism in skin and thus played its therapeutic effects.

Importantly, *ABCA6*, a gene that encodes a cholesterol transporter and belongs to the superfamily of ABC transporters, was significantly upregulated in treated *Z9* pigs (Figure 6H), and it was confirmed by RT-qPCR. RT-qPCR results showed no change in the expression level of *ABCA8* and *ABCA9* after acitretin treatment (Supplementary Figure S7A). Furthermore, acitretin was demonstrated to trigger *ABCA6* expression *in vitro* using HaCat cells cultured in the present of acitretin for 60 h (Supplementary Figure S7B). In brief, we inferred that the triggered expression of *ABCA6* may partially compensate the loss of function of *ABCA12*, as a mechanism that how acitretin work in treating HI in human beings and pigs.

Discussion

We have successfully established a systematic three-generation ENU mutagenesis porcine program and screened a large scale of mutants with a broad range of phenotypes that could be potentially developed into models for human diseases (Hai et al., 2017a, 2017b; Zhang et al., 2017). Forward genetic screening is an important method that can be used to establish human disease models and to facilitate studies of gene function (Hrabé de Angelis and Balling, 1998) due to the advantages like high throughput and identification of novel molecular signal pathways without prior hypothesis (de Bruijn et al., 2009). ENU mutagenesis generates a series of point mutations that frequently mimic the subtlety and heterogeneity of human genetic lesions (Funato et al., 2016; Oliver and Davies, 2012). Pigs are increasingly being used as human disease models due to their anatomical and physiological similarities with human and many breeding and handling advantages (Swindle et al., 2012). Most dominantly, porcine skin more closely resembles human skin than rodent skin, making pigs a better model to study skin-related disease.

In this study, we report the discovery of a novel mutation (*ABCA12* IVS49-727 A>G) in Bama miniature pigs induced by ENU mutagenesis, which led to a remarkable model of human HI. The IVS49-727 A>G mutation mainly results in a splicing alteration with a 132-nt insertion between exon 49 and exon 50, introducing a premature stop codon in the *ABCA12* gene. It is consistent with human HI findings that only truncation or conserved region deletion mutations could seriously affect ABCA12 protein function and lead to the HI phenotype (Akiyama et al., 2005). Moreover, up to 13% (5 in 38) of the reported *ABCA12* mutations in human HI are splice site mutations (Rajpopat et al., 2011). Therefore, future gene therapy aiming at splice site mutations should be feasible for human. The IVS49-727 A>G mutation happen to generate a typical restriction of 5′ consensus sequence of intron (from ATAAGT to GTAAGT; Qian et al., 2014); as a result, *ABCA12* pre-mRNA of *Z9* pig shows abnormal splicing. Therefore, targeting the sequence including this 6-nt sequence by genome editing tool should be an effective treatment method to restore the abnormal alternative splicing. Interestingly, extremely low level of *ABCA12* WT transcript, generated by alternative splicing, was observed in *Z9* skin. However, despite of the expression of WT transcript, the phenotype cannot be recovered in *Z9* pigs.

The *Z9* pigs perfectly mimic the clinical manifestations of human patients with HI, including hyperkeratosis, ectropion, eclabium, developmental delay, abnormal LGs, anomalous skin barrier function, lower birth weight, and defects in lipid metabolism, which provide us a valuable model to understand the pathological mechanism of HI. A disordered arrangement of spinous cells and basale cells was observed in *Z9* pig epidermis but has not been reported in *ABCA12* null mouse epidermis. However, these findings are similar to those seen in skin biopsy of human patients with HI, which exhibited disordered basale cells (Rathore et al., 2015). Therefore, we infer that epidermal disordered arrangement is one of the common features between human patients with HI and *Z9* pigs. Ki67 staining showed that imbalanced cell proliferation in the SB might result in disordered basale cells of the skin from *Z9* pigs.

Previous lipidomics studies in the skin of *ABCA12* null mice led to conflicting results (Smyth et al., 2008; Zuo et al., 2008). Smyth et al. showed that Cer was significantly increased in the skin of *ABCA12* null mice, while the study from Zou et al. showed that Cer was decreased. Our results of lipidomics analysis in pigs were consistent with the view that Cer was significantly increased in *ABCA12* mutant skin. These data certainly demonstrate that the *ABCA12* mutation impairs its transporter activity and the accumulated Cer results in detrimental effects to skin keratinization.

We observed that *Z9* epidermis exhibited premature apoptosis by TUNEL assay. It was reported that mutations of *ABCA12* gene would result in Cer accumulation in the cytoplasm (Smyth et al., 2008), which may inhibit the activation of AKT (Bourbon et al., 2002). Akt pathway is an essential pathway for cell survival and growth during development, and it is well known that inactivation of AKT promotes apoptosis (Brunet et al., 1999). In the current study, the inactivation AKT in *Z9* skin was observed and may be resulted from the Cer accumulation. These results indi-

cated that AKT plays an antiapoptotic role in ABCA12-deficient keratinocytes.

The *ABCA12* null mice die shortly after birth, and retinoid therapy to the pregnant mice failed to improve the pups' skin phenotype or extend the survival period of the *ABCA12* defective newborns (Yanagi et al., 2008). In contrast, *Z9* pigs showed remarkable therapeutic effects with the acitretin treatment, a drug commonly used clinically to increase the survival rate of patients with HI. The drug enters the cells by nonreceptor-mediated endocytosis, and once in the nucleus, acitretin activates two classes of nucleic acid receptors—retinoic acid receptors (RAR) and retinoid X receptors (RXR)—which subsequently activate expression of their downstream genes (Dogra and Yadav, 2014). Acitretin has multiple effects on epidermal cell growth and differentiation through induction of epidermal growth factor and transforming growth factor β (Tong et al., 1990). However, the exact mechanism of the acitretin effects on HI remains unknown. *Z9* pigs offer the potential of studying the mechanisms of acitretin treatment and possibility of improving therapies of human HI.

Among the top DEGs identified by RNA-seq, *STRA6, RBP1,* and *RARB* play roles in retinoid metabolism, and upregulation of these genes indicated that administration of acitretin to pregnant sow and neonatal pigs has induced a therapeutic response in skin cells of Z9 pigs. The analysis of genes clustered in epidermis development and cornification shows that acitretin treatment in *Z9* pigs gained improvement in the skin phenotype through alleviation of skin cornification. These results confirmed that the clinical improvement of acitretin patients might be obtained via the activation of RAR and RXR. The upregulated epidermis development of *Z9* pigs was identified by the functional enrichment analysis, while genes in GO term of cornification were significantly downregulated after acitretin treatment in *Z9* pigs, which might explain the therapeutic mechanism of acitretin in treating HI. Besides, ABCA6, a transporter of cholesterol that belongs to ABCA family, was significantly upregulated by acitretin treatment, suggesting that ABCA6 might play a role through the compensation of function loss of *ABCA12* gene. These results provide new insights for explaining the therapeutic mechanism of acitretin.

In summary, we have generated a novel HI pig model based on a deep intronic mutation in *ABCA12*. This pig model faithfully replicates the abnormalities and pathologies seen in human patients and shows positive responses to acitretin treatment. This model provides a useful tool for understanding the disease development and a new material for developing treatments strategies.

Materials and methods

Animals

Bama miniature pigs were raised at the Beijing Farm Animal Research Center (attached to Institute of Zoology, Chinese Academy of Sciences), where *ad libitum* access to feed and water is supplied during the experimental period. All experiments involving animals were performed according to the guidelines for the Care and Use of Laboratory Animals established by the Beijing Association for Laboratory Animal Science and were approved by the Animal Ethics Committee of the Institute of Zoology, Chinese Academy of Sciences.

Skin permeability assay and gravimetric TEWL assay

In situ skin permeability assays were performed with toluidine blue as previously described (Hardman et al., 1998). WT and *Z9* pigs were euthanized after birth and the entire bodies were washed with PBS, incubated in 0.1% toluidine blue for 5 min, washed with PBS three times, and then photographed.

TEWL assay was performed on samples harvested from the neonatal dorsal skin, which is able to measure the water evaporation from the skin surface. Skin samples sealed on laboratory film (Bemis) with Vaseline were weighed on a microbalance every 30 min for 5 h at ambient temperature. Each skin sample was photographed and the areas were calculated with imageJ software. TEWL was calculated as milligrams of water loss per square millimeter of epidermis per hour.

Gene mapping analysis of Z9 pigs

Twenty-four genomic DNA samples (including the G1 founder, three G2 female pigs, 12 G3 WT pigs, and eight G3 affected pigs) were isolated from ear skin tissues using a phenol–chloroform method. DNA samples were subjected to whole-genome single-nucleotide polymorphism (SNP) genotyping using a porcine SNP60 BeadChips (Illumina), which contains 62163 SNP markers. Raw genotype data were processed using standard quality control procedures. A family-based GWAS (transmission disequilibrium test analysis) was performed to detect SNP loci showing a significant association with the *Z9* trait using PLINK software (Purcell et al., 2007). Additionally, Merlin software (Abecasis et al., 2002) was also used to conduct a parametric linkage analysis based on an autosomal recessive model, and the logarithm of the odds (LOD) score was calculated to assess the evidence for linkage.

Identification of causative mutation

Sanger sequencing of all CDSs of 53 exons and intronic sequence of intron 49 in *ABCA12* gene was performed. All primers used in this paper are available in Supplementary Table S2.

Minigene assay

To construct minigenes, genomic sequence of *ABCA12* ranging from exon 49 to 50 were amplified by PCR with DNA template from WT and *Z9* pigs. Forward primer (*Hin*dIII): 5′-ACTAAGCTTACAGGGTGTCAACTTCAGTGAG-3′. Reverse primer (*Xho*I): 5′-ACTCTCGAGAGGCGAGTATGGTACTGTGGG-3′. WT and *Z9* PCR products were digested with HindIII and XhoII and then cloned into pcDNA3.1 vector. For each minigene experiment, 2.5 μg minigene vectors were transfected to 293T cells. After

24 h, the cells were collected for RNA isolation and reverse-transcription PCR using M-MLV reverse transcriptase (Promega). Transcription products of the minigenes were amplified with universal primers T7 and BGH and then subjected to Sanger sequencing.

Lipid accumulation assay

Fibroblasts were cultured from ear skin tissues of the *ABCA12*$^{+/+}$, *ABCA12*$^{+/Z9}$, and *ABCA12*$^{Z9/Z9}$ pigs. Assays of lipid accumulation were performed according to instruction previously described (Smyth et al., 2008). Fibroblasts were incubated in serum-containing medium with TO-901317 (4 mM; Cayman Chemical) and AcLDL (10 mg/ml; Yeasen Biotech) for 18 hrs. Fibroblasts were washed with PBS, fixed with 4% formaldehyde, and then stained with Oil Red O (Sigma-Aldrich) working solution.

Acitretin therapeutic trials

Pregnant pigs were administered orally with acitretin (Huapont Pharm; 1 or 10 mg/kg daily) 30 days before parturition, and newborn piglets were dosed orally with acitretin (1 mg/kg daily) soon after birth.

Deep sequencing and reads mapping

RNA-seq analysis was conducted at Annoroad Gene Technology. Paired-end libraries for sequencing were prepared according to the Illumina PE library preparation protocol (Illumina), and the qualified libraries were sequenced on an Illumina Hiseq 2500 sequencing platform. The qualified reads (clean reads) were aligned to the pig built 11.1 reference sequence using TopHat software with default parameters. The BAM files (generated from TopHat) that contained the read alignments were then used to evaluate gene expression levels by fragments per kilobaseof exon per million fragments mapped (FPKM) values using Cufflinks software.

DEG identification

To identify the gene expression level changes, the number of the uniquely mapped reads assigned to each gene in the pig genome (using the gene annotation file for pigs 'Sus_scrofa.Sscrofa11.1.94.gtf') was first analyzed using the featureCounts package. The read counts of each gene were used as input and the differentially expressed genes in different groups with a threshold value of FDR <0.05 and a fold change ≥ 2 were identified by edgeR software.

Clustering analysis and GO analysis

The hierarchical clustering of DEGs was performed using the heatmap.2 function in gplots, and a heatmap was generated to represent the gene clusters showing similar expression patterns. GO enrichment analysis of upregulated and downregulated genes was performed using the Metascape toolkits. The GO terms with *P*-values (enrichment score) <0.05 were regarded as 'statistically significant'.

Statistics

All data are expressed as mean $\pm$ standard deviation (SD). Student's *t*-test was used for all analyses, and statistical significance was defined as *P*-value <0.05. The replicates in each analysis can be found in the figure legends.

Supplementary material

Supplementary material is available at *Journal of Molecular Cell Biology* online.

Acknowledgements

The authors thank all the personnel at the Beijing Farm Animals Research Center, the Chinese Academy of Sciences, and the Chinese Swine Mutagenesis Consortium whose names are not listed as coauthors of this paper for their assistance.

Funding

This work was supported by the Strategic Priority Research Programs of CAS (XDA16030300), the National Natural Science Foundation of China (81671274, 31272440, and 31801031), the National Transgenic Project of China (2016ZX08009003-006-007), and the Elite Youth Program of the Chinese Academy of Agricultural Sciences (ASTIP-IAS05).

Conflict of interest: none declared.

References

Abdullahi, A., Amini-Nik, S., and Jeschke, M.G. (2014). Animal models in burn research. Cell. Mol. Life Sci. *71*, 3241–3255.

Abecasis, G.R., Cherny, S.S., Cookson, W.O., et al. (2002). Merlin—rapid analysis of dense genetic maps using sparse gene flow trees. Nat. Genet. *30*, 97–101.

Akiyama, M. (2010). ABCA12 mutations and autosomal recessive congenital ichthyosis: a review of genotype/phenotype correlations and of pathogenetic concepts. Hum. Mutat. *31*, 1090–1096.

Akiyama, M., and Shimizu, H. (2008). An update on molecular aspects of the non-syndromic ichthyoses. Exp. Dermatol. *17*, 373–382.

Akiyama, M., Sugiyama-Nakagiri, Y., Sakai, K., et al. (2005). Mutations in lipid transporter ABCA12 in harlequin ichthyosis and functional recovery by corrective gene transfer. J. Clin. Invest. *115*, 1777–1784.

Allikmets, R., Gerrard, B., Hutchinson, A., et al. (1996). Characterization of the human ABC superfamily: isolation and mapping of 21 new genes using the expressed sequence tags database. Hum. Mol. Genet. *5*, 1649–1655.

Annilo, T., Shulenin, S., Chen, Z.Q., et al. (2002). Identification and characterization of a novel ABCA subfamily member, ABCA12, located in the lamellar ichthyosis region on 2q34. Cytogenet. Genome Res. *98*, 169–176.

Ansell, D.M., Holden, K.A., and Hardman, M.J. (2012). Animal models of wound repair: are they cutting it? Exp. Dermatol. *21*, 581–585.

Barbero, A.M., and Frasch, H.F. (2009). Pig and guinea pig skin as surrogates for human in vitro penetration studies: a quantitative review. Toxicol. In Vitro *23*, 1–13.

Bourbon, N.A., Sandirasegarane, L., and Kester, M. (2002). Ceramide-induced inhibition of Akt is mediated through protein kinase $C\zeta$: implications for growth arrest. J. Biol. Chem. *277*, 3286–3292.

de Bruijn, E., Cuppen, E., and Feitsma, H. (2009). Highly efficient ENU mutagenesis in zebrafish. Methods Mol. Biol. *546*, 3–12.

Brunet, A., Bonni, A., Zigmond, M.J., et al. (1999). Akt promotes cell survival by phosphorylating and inhibiting a Forkhead transcription factor. Cell *96*, 857–868.

Dean, M., and Allikmets, R. (2001). Complete characterization of the human ABC gene family. J. Bioenerg. Biomembr. *33*, 475–479.

Debeer, S., Le Luduec, J.B., Kaiserlian, D., et al. (2013). Comparative histology and immunohistochemistry of porcine versus human skin. Eur. J. Dermatol. *23*, 456–466.

Dogra, S., and Yadav, S. (2014). Acitretin in psoriasis: an evolving scenario. Int. J. Dermatol. *53*, 525–538.

Farhadi, R., and Kazemi, S.H. (2013). Harlequin ichthyosis in a neonate born with assisted reproductive technology: a case report. Med. J. Islam. Repub. Iran *27*, 229–232.

Funato, H., Miyoshi, C., Fujiyama, T., et al. (2016). Forward-genetics analysis of sleep in randomly mutagenized mice. Nature *539*, 378–383.

Hai, T., Cao, C., Shang, H., et al. (2017a). Pilot study of large-scale production of mutant pigs by ENU mutagenesis. eLife *6*, e26248.

Hai, T., Guo, W., Yao, J., et al. (2017b). Creation of miniature pig model of human Waardenburg syndrome type 2A by ENU mutagenesis. Hum. Genet. *136*, 1463–1475.

Hardman, M.J., Sisi, P., Banbury, D.N., et al. (1998). Patterned acquisition of skin barrier function during development. Development *125*, 1541–1552.

Hrabé de Angelis, M., and Balling, R. (1998). Large scale ENU screens in the mouse: genetics meets genomics. Mutat. Res. *400*, 25–32.

Kelsell, D.P., Norgett, E.E., Unsworth, H., et al. (2005). Mutations in ABCA12 underlie the severe congenital skin disease harlequin ichthyosis. Am. J. Hum. Genet. *76*, 794–803.

Koch, P.J., de Viragh, P.A., Scharer, E., et al. (2000). Lessons from loricrin-deficient mice: compensatory mechanisms maintaining skin barrier function in the absence of a major cornified envelope protein. J. Cell Biol. *151*, 389–400.

Lefévre, C., Audebert, S., Jobard, F., et al. (2003). Mutations in the transporter ABCA12 are associated with lamellar ichthyosis type 2. Hum. Mol. Genet. *12*, 2369–2378.

Lin, J., Cao, C., Tao, C., et al. (2017). Cold adaptation in pigs depends on UCP3 in beige adipocytes. J. Mol. Cell Biol. *9*, 364–375.

Meurens, F., Summerfield, A., Nauwynck, H., et al. (2012). The pig: a model for human infectious diseases. Trends Microbiol. *20*, 50–57.

Oliver, P.L., and Davies, K.E. (2012). New insights into behaviour using mouse ENU mutagenesis. Hum. Mol. Genet. *21*, R72–R81.

Parikh, K., Brar, K., Glick, J.B., et al. (2016). A case report of fatal harlequin ichthyosis: insights into infectious and respiratory complications. JAAD Case Rep. *2*, 301–303.

Purcell, S., Neale, B., Todd-Brown, K., et al. (2007). PLINK: a tool set for whole-genome association and population-based linkage analyses. Am. J. Hum. Genet. *81*, 559–575.

Qian, X., Ba, Y., Zhuang, Q., et al. (2014). RNA-seq technology and its application in fish transcriptomics. OMICS *18*, 98–110.

Rajpopat, S., Moss, C., Mellerio, J., et al. (2011). Harlequin ichthyosis: a review of clinical and molecular findings in 45 cases. Arch. Dermatol. *147*, 681–686.

Rathore, S., David, L.S., Beck, M.M., et al. (2015). Harlequin ichthyosis: prenatal diagnosis of a rare yet severe genetic dermatosis. J. Clin. Diagn. Res. *9*, Qd04–Qd06.

Sakai, K., Akiyama, M., Sugiyama-Nakagiri, Y., et al. (2007). Localization of ABCA12 from Golgi apparatus to lamellar granules in human upper epidermal keratinocytes. Exp. Dermatol. *16*, 920–926.

Singh, S., Bhura, M., Maheshwari, A., et al. (2001). Successful treatment of harlequin ichthyosis with acitretin. Int. J. Dermatol. *40*, 472–473.

Smyth, I., Hacking, D.F., Hilton, A.A., et al. (2008). A mouse model of harlequin ichthyosis delineates a key role for Abca12 in lipid homeostasis. PLoS Genet. *4*, e1000192.

Steinert, P.M., and Marekov, L.N. (1995). The proteins elafin, filaggrin, keratin intermediate filaments, loricrin, and small proline-rich proteins 1 and 2 are isodipeptide cross-linked components of the human epidermal cornified cell envelope. J. Biol. Chem. *270*, 17702–17711.

Summerfield, A., Meurens, F., and Ricklin, M.E. (2015). The immunology of the porcine skin and its value as a model for human skin. Mol. Immunol. *66*, 14–21.

Swindle, M.M., Makin, A., Herron, A.J., et al. (2012). Swine as models in biomedical research and toxicology testing. Vet. Pathol. *49*, 344–356.

Tong, P.S., Horowitz, N.N., and Wheeler, L.A. (1990). Trans retinoic acid enhances the growth response of epidermal keratinocytes to epidermal growth factor and transforming growth factor β. J. Invest. Dermatol. *94*, 126–131.

Yanagi, T., Akiyama, M., Nishihara, H., et al. (2008). Harlequin ichthyosis model mouse reveals alveolar collapse and severe fetal skin barrier defects. Hum. Mol. Genet. *17*, 3075–3083.

Yanagi, T., Akiyama, M., Nishihara, H., et al. (2011). AKT has an anti-apoptotic role in ABCA12-deficient keratinocytes. J. Invest. Dermatol. *131*, 1942–1945.

Yoneda, K., and Steinert, P.M. (1993). Overexpression of human loricrin in transgenic mice produces a normal phenotype. Proc. Natl Acad. Sci. USA *90*, 10754–10758.

Zhang, Y., Xue, Y., Cao, C., et al. (2017). Thyroid hormone regulates hematopoiesis via the TR–KLF9 axis. Blood *130*, 2161–2170.

Zuo, Y., Zhuang, D.Z., Han, R., et al. (2008). ABCA12 maintains the epidermal lipid permeability barrier by facilitating formation of ceramide linoleic esters. J. Biol. Chem. *283*, 36624–36635.